

1 **Effects of decreased Rac activity and malignant state on oral squamous cell**
2 **carcinoma**

3

4 Hani Al-Shareef¹, Yudai Matsuoka², Mikihiko Kogo², and Hirokazu Nakahara^{1,2*}

5

6 ¹Department of Oral & Maxillofacial Surgery, Osaka City University Graduate School
7 of Medicine, Osaka, Osaka, Japan

8 ²The First Department of Oral & Maxillofacial Surgery, Osaka University Graduate
9 School of Dentistry, Suita, Osaka, Japan

10

11 Short title: Effects of Rac Inhibition on oral SCC

12

13 *Corresponding author:

14 Hirokazu Nakahara

15 Department of Oral & Maxillofacial Surgery

16 Osaka City University Graduate School of Medicine

17 Osaka 545-8585, Japan

18 Telephone: +816-6645-2781

19 Fax: +816-6646-6063

20 E-mail: nakahara.hirokazu@med.osaka-cu.ac.jp

22 **Abstract**

23 Rac proteins, members of the Rho family of small GTP-binding proteins, have been
24 implicated in transducing a number of signals for various biological mechanisms,
25 including cell cytoskeleton organization, transcription, proliferation, migration, and
26 cancer cell motility. Among human cancers, Rac proteins are highly activated by either
27 overexpression of the genes, up-regulation of the protein, or by mutations that allow the
28 protein to elude normal regulatory signaling pathways. Rac proteins are involved in
29 controlling cell survival and apoptosis. The effects of Rac inhibition by the Rac-specific
30 small molecule inhibitor NSC23766 or by transfection of dominant negative Rac (Rac-
31 DN) were examined on three human-derived oral squamous cell carcinoma cell lines
32 that exhibit different malignancy grades, OSC-20 (grade 3), OSC-19 (grade 4C), and
33 HOC313 (grade 4D). Upon suppression of Rac, OSC-19 and HOC313 cells showed
34 significant decreases in Rac activity and resulted in condensation of the nuclei and up-
35 regulation of c-Jun N-terminal kinase (JNK), leading to caspase-dependent apoptosis. In
36 contrast, OSC-20 cells showed only a slight decrease in Rac activity, which resulted in
37 slight activation of JNK and no change in the nuclei. Fibroblasts treated with
38 NSC23766 also showed only a slight decrease in Rac activity with no change in the
39 nuclei or JNK activity. Our results indicated that apoptosis elicited by the inhibition of
40 Rac depended on the extent of decreased Rac activity and the malignant state of the
41 squamous cell carcinoma. In addition, activation of JNK strongly correlated with
42 apoptosis. Rac inhibition may represent a novel therapeutic approach for cancer
43 treatment.

44 **Keywords:** Rac, apoptosis, JNK, anti-cancer therapy

46 **Introduction**

47 Rac proteins have been implicated in transducing a variety of signal pathways that are
48 essential for cell function [1–4]. Upon stimulation by growth factors, Rac proteins are
49 activated through a tightly regulated guanosine diphosphate/guanosine triphosphate
50 (GDP/GTP) cycle. Activated Rac proteins are a key regulator of a number of cell
51 activities, such as cell organization of the cytoskeleton, transcription, cell proliferation,
52 cell migration, and cancer cell motility [5,6]. Rac proteins are also involved in
53 controlling cell survival and apoptosis [7]. Activation of the Rac family induces a strong
54 signal to activate cancer cells and related fibroblasts in the apoptosis mechanism [8–11].
55 In most human cancers, Rac proteins are highly activated by either overexpression of
56 the gene, up-regulation of the protein, or mutations that allow the protein to elude
57 normal regulatory signaling pathways [12–15]. However, the mechanisms of Rac
58 GTPases and their relation to apoptosis require additional studies, which could
59 contribute toward their development as therapeutic agents in cancer treatment.

60 Activation of c-Jun N-terminal kinase (JNK) by various stimulatory signals results in
61 an apoptotic response via a number of its substrate effectors. Many studies have
62 indicated that Rac is an upstream activator of JNK/c-Jun signaling [9,16,17] and others
63 have recently reported that Rac can also suppress the JNK signaling pathway [10–18].

64 In the current study, we investigated the role of Rac in the malignant oral squamous
65 carcinoma cell lines OSC-20, OSC-19, and HOC313. We found that apoptosis induced
66 by the inhibition of Rac was dependent on the extent of decreased Rac activity and the
67 malignant state of the squamous cell carcinoma. We also determined that activation of
68 JNK strongly correlated with the induced apoptosis.

69

70 **Results**

71 **Characterization of three human-derived oral squamous cell carcinoma cell lines,**

72 **OSC-20, OSC-19, and HOC313 cells**

73 The three cell lines used in the current study, OSC-20, OSC-19, and HOC313 cells,

74 were derived from human oral squamous cell carcinomas and each demonstrates

75 different malignancy according to Yamamoto-Kohama's (Y-K) classification [19].

76 OSC-20 cells are classified as grade 3, OSC-19 as grade 4C, and HOC313 as grade 4D.

77 To characterize each cell type, the cells were cultured on microscope coverslips and

78 stained with rhodamine-phalloidin. As shown in Fig 1A, OSC-20 cells formed

79 lamellipodia, OSC-19 cells formed filopodia, and HOC313 cells formed abundant

80 horizontal growth stress fibers with microspikes. To further investigate the

81 characteristics of each cell, we then examined the cytoskeletal proteins of three cell

82 lines. OSC-19 cells stained positive for E-cadherin and cytokeratin (Fig 1B). On the

83 other hand, HOC313 stained positive for N-cadherin and vimentin (Fig 1B). As shown

84 in Fig 1B, OSC-20 cells showed staining for E-cadherin and N-cadherin, cytokeratin,

85 and vimentin. These results indicated that OSC-19 cells had epidermal characteristics

86 and HOC313 cells had mesenchymal characteristics. OSC-20 cells were characterized

87 as an intermediate between OSC-19 and HOC313 cells.

88

89 **Fig 1. Characteristics of three human-derived oral squamous cell carcinoma cell**

90 **lines, OSC-20, OSC-19, HOC313 cells, and fibroblasts.** All cells were seeded onto

91 coverslips and grown in DMEM containing 10% fetal bovine serum and 5% Nu-serum

92 Growth Medium Supplement for 24 h and then stained with rhodamine-phalloidin to

93 compare morphology.

94

95

96 **Inhibition of Rac activity induced cell death in OSC-19 and HOC313 cells but not**
97 **in OSC-20 cells or fibroblasts**

98 Based on the molecular evidence that Rac activity increases as a mechanism of cancer,
99 we hypothesized that inhibition of Rac might be detrimental to tumor cells. To test this
100 hypothesis, we evaluated the effects of the selective Rac1 inhibitor NSC23766 on OSC-
101 20, OSC-19, and HOC313 cells. Impressively, OSC-19 and HOC313 cell lines treated
102 with 100 μ M NSC23766 for 24 h showed morphological changes indicative of cell
103 death whereas the OSC-20 cell line failed to show morphological changes associated
104 with cell death (Fig 2). Furthermore, similar to the OSC-20 cells, fibroblasts treated
105 with 100 μ M NSC23766 for 24 h also showed no cell death related morphology (Fig 2).
106 We performed western blot analysis of pull-down assays for the whole Rac protein and
107 a Rac effector domain to evaluate any changes or association differences in Rac activity
108 among the three SCC cell lines and fibroblasts. Based on the results, the Rac expression
109 in general was obvious in the OSC-20, OSC-19, and HOC313 cell lines and the Rac
110 pull-down assay revealed a high level of Rac activity, more than that in the fibroblasts
111 under the untreated condition (Fig 3). These data suggested that Rac was overexpressed
112 and had a higher level of activity in OSC-20, OSC-19, and HOC313 cell lines compared
113 with those in the fibroblasts. Moreover, a significant decrease in Rac activity was also
114 observed in all the cell lines after treatment with NSC23766 (Fig 3). However, the
115 extent of decreased Rac activity in OSC-19 and HOC313 cells was greater than that of
116 OSC-20 cells and fibroblasts (Fig 3).

117

118

119 **Fig 2. Phase-contrast micrographs demonstrating the effects of the selective Rac1**
120 **inhibitor NSC23766 on OSC-20, OSC-19, HOC313, and fibroblast cells.** All cells
121 were treated with 100 μ M NSC23766 for 24 h. OSC-19 and HOC313 cells showed
122 morphological changes associated with cell death, in contrast to OSC-20 cells and
123 fibroblasts, which did not demonstrate morphological changes.

124

125 **Fig 3. Western blot analyses of pull-down assays for the whole Rac protein and a**
126 **Rac effector domain.** The extent of decreased Rac activity in OSC-19 and HOC313
127 cells was more significant than that in OSC-20 cells and fibroblasts. The three human-
128 derived oral squamous cell carcinoma cell lines (OSC-20, OSC-19, HOC313), and
129 fibroblasts were treated with 0, 50, or 100 μ M selective Rac1 inhibitor NSC23766 and
130 incubated them for 9 h in serum followed by the transient transfection with the
131 dominant negative Rac (Rac-DN) for 48 h. Pull down the GTP-loaded Rac from the
132 total protein lysates was performed using a Rac1 Activation Kit (GST-human Pak1-
133 PBD) according to the manufacturer's instructions.

134

135

136 **The type of cell death elicited by inhibition of Rac activity was apoptosis**
137 After treating the SCC cells and fibroblasts with 100 μ M NSC23766 to inhibit Rac
138 activity and staining the nuclei with 4',6-diamidino-2-phenylindole (DAPI) stain, we
139 examined the cells under a microscope and checked their structure to determine whether
140 the cell death had occurred due to necrosis or apoptosis. We observed morphological
141 characteristics of apoptosis, such as cell shrinkage, nuclear condensation, and

142 fragmentation in the OSC-19 and HOC313 cells (Fig 4A). In contrast, these findings
143 were not seen in the OSC-20 cells or fibroblasts after they were treated with the same
144 procedure (Fig 4A). We also performed a cell death detection enzyme-linked
145 immunosorbent assay (ELISA) to confirm our results regarding the apoptotic cell death
146 (Fig 4B). The results revealed a significant 2–6-fold increase in apoptosis in OSC-19
147 and HOC313 cells after treatment with NSC23766 compared to the control cells, OSC-
148 20 cells, and fibroblasts after treatment ($p < 0.05$). These results suggested that the
149 inhibition of Rac activity by the Rac-specific small molecule inhibitor NSC23766 had a
150 significant role in inducing apoptosis in the OSC-19 and HOC313 cells. To extend these
151 findings, we performed additional investigations into the mechanism of inhibition of
152 Rac activity. Briefly, the cells were transfected with an expression vector encoding a
153 Myc-tagged Rac dominant negative mutant (Rac-DN) and the expression levels were
154 measured in the treated cells. The Rac-DN transformed cell showed cell shrinkage,
155 nuclear condensation, and fragmentation in the cell nuclei (Fig 4A). To confirm our
156 results regarding apoptotic cell death in the transformed cells, we then performed cell
157 death detection ELISA assay (Fig 4B). The amount of cell death resulting from
158 apoptosis for the cells treated with Rac-DN appeared less than that observed for the
159 cells treated with 100 μ M NSC23766. Analytical evaluation of the results revealed a
160 negative correlation, which was reasonable since the transfection efficiency was
161 approximately 30–40% and a small amount of Rac activity was detected in Rac pull-
162 down assays of cells that underwent the transient expression with Rac-DN (Fig 3).
163 Overall, these results suggested that the inhibition of Rac activity was likely to lead to
164 the cell apoptosis in OSC-19 and HOC313 cells, which was in contrast to OSC-20 cells
165 or fibroblasts in which no cell apoptosis was observed.

166

167

168 **Fig 4. DAPI staining of nuclei and cell death detection ELISA assay.** (A) The three
169 human-derived oral squamous cell carcinoma cell lines, OSC-20, OSC-19, and
170 HOC313, and human fibroblasts were seeded onto round glass coverslips glass (10^5
171 cells). The cells were experimentally treated and then fixed in 4% paraformaldehyde,
172 washed, and stained with DAPI for 1 h at room temperature. The cells were treated with
173 selective Rac1 inhibitor NSC23766 (100 μ M) for 9 h, then underwent transient
174 transfection with an expression vector of a dominant negative Rac (Rac-DN).
175 Fibroblasts were treated with NSC23766 (100 μ M) under the same conditions. (B) A
176 cell death detection ELISA assay was performed according to the manufacturer's
177 instructions to confirm the results regarding the apoptotic cell death.

178

179

180 **Hyper-phosphorylation of JNK correlated with apoptosis induced by the inhibition**
181 **of Rac**

182 Studies have suggested that Rac acts as an upstream activator of JNK/c-Jun signaling
183 [9,16,17], while others have suggested that Rac can also suppress the JNK pathway
184 [10,18]. To expand our current studies related to the inhibition of Rac activity and its
185 relation to apoptosis in OSC-19 and HOC313 cells, we investigated downstream
186 signaling of the Rac pathway. We briefly inhibited the Rac activity by treating the cells
187 with 100 μ M NSC23766 for 9 h and the examined the phosphorylation of JNK. We
188 detected hyper-phosphorylation of JNK, as assessed by a phospho-specific antibody
189 (Fig 5A). In contrast, OSC-20 cells treated with 100 μ M NSC23766 under the same

190 conditions showed only slight activation of JNK. Furthermore, there was no difference
191 detected in JNK activity for fibroblasts after being treated under the same circumstances
192 (Fig 5A).

193

194

195 **Fig 5. (A)** Western blot analysis of JNK using anti-JNK and pJNK polyclonal
196 antibodies and a β -actin monoclonal antibody. Rac activity was inhibited by treating the
197 human-derived oral squamous cell carcinoma cell lines OSC-19, OSC-20, and HOC313
198 with 100 μ M selective Rac1 inhibitor NSC23766 for 9 h followed by the transient
199 transfection of the three cell lines with a dominant negative Rac (Rac-DN) for 48 h. The
200 phosphorylation of JNK was examined. Fibroblasts were treated with NSC23766 (100
201 μ M) under the same conditions. **(B)** Phase-contrast micrographs. OSC-19 and HOC313
202 cells were pretreated with JNK-specific inhibitor (20 μ M SP600125) for 1 h before
203 treatment with 100 μ M NSC23766 for 24 h. **(C)** DAPI staining of nuclei to detect
204 morphological changes. OSC-19 and HOC313 cells were seeded onto coverslips, the
205 cells were experimentally treated, and fixed in 4% paraformaldehyde, washed and
206 stained with DAPI for 1 h at room temperature. The DAPI-stained cells were then
207 pretreated with JNK-specific inhibitor (20 μ M SP600125) for 1 h before treatment with
208 the 100 μ M NSC23766 for 9 h. Cell death was detected by an ELISA assay according to
209 the manufacturer's instructions to confirm our results regarding the apoptotic cell death.

210

211

212 To further confirm whether the inhibition of Rac activity in relation to apoptosis was
213 mediated through a JNK-upregulation mechanism, we pretreated the OSC-19 and

214 HOC313 cells with the JNK-specific inhibitor SP600125 (20 μ M) for 1 h prior to
215 treating the cells with NSC23766 [19-20] and evaluated the effect on apoptosis. The
216 cells failed to show hallmarks of cell-death, even after 24 h of incubation with 100 μ M
217 NSC23766 (Fig 5B). Treating the cells with SP600125 prevented the condensation and
218 fragmentation of the cell nuclei and analysis using the cell death detection ELISA assay
219 showed that apoptosis was decreased by approximately 50% (Fig 5C). In conclusion,
220 these results suggested that the activation of JNK was more effective after inhibition of
221 Rac activity in OSC-19 and HOC313 cells compared to OSC-20 cells and fibroblasts
222 and was necessary for the induction of apoptosis.

223

224 **Discussion**

225 In particular, several lines of evidence indicate that Rac proteins play crucial roles in
226 several aspects of cell survival and apoptosis [7,21]. Therefore, inhibition of Rac using
227 specific inhibitors may allow for the modulation of apoptosis [6]. In the current study, a
228 couple key included: (a) inhibition of Rac activity and its mediated downstream
229 signaling likely led to the cell apoptosis observed for the OSC-19 and HOC313 cells,
230 but not for the OSC-20 cells or fibroblasts; (b) the activation of JNK signaling in OSC-
231 19 and HOC313 cells was associated with the inhibition of Rac activity and thereby to
232 apoptosis. Consequently, activation of the Rac pathway may indicate the preservation of
233 cancer cell progression and the selective inhibition of Rac activity may trigger apoptosis
234 in cancer cells. Therefore, inducing apoptosis in cancer cells by inhibiting Rac activity
235 may be exploited as a novel treatment for cancer. However, Rac activity was more
236 readily suppressed in OSC-19 and HOC313 cells compared to OSC-20 cells and
237 fibroblasts suggesting potential variation in response to treatment.

238 One mechanism that requires additional elucidation is the regulation of JNK activity
239 after suppression of Rac. Many studies have indicated that Rac acts as an upstream
240 activator of JNK signaling in certain cells [9,16,17], while others have reported that Rac
241 can suppress the JNK pathway [10,18]. In general, whether Rac positively or negatively
242 regulates the JNK pathway may primarily depends on the specific cancer cell type.

243 It is important to emphasize that the hyper-phosphorylation of JNK was activated by
244 the inhibition of Rac activity in OSC-19 and HOC313 cells by treating the cells with
245 100 μ M NSC23766, but this activation of JNK did not occur in OSC-20 cells or
246 fibroblasts. Moreover, the suppression of JNK activity by treating the OSC-19 and
247 HOC313 cells with a JNK-specific inhibitor induced similar effects on apoptosis as the
248 direct inhibition of Rac. Taken together, these findings suggest that the activation of
249 JNK was more effective after treatment to inhibit Rac activity in OSC-19 and HOC313
250 cells compared to OSC-20 cells and fibroblasts and that JNK activation was necessary
251 for induction of apoptosis.

252 In conclusion, results from our study suggest that the inhibition of Rac activity
253 resulted in the hyper activation of JNK, which led to apoptosis in OSC-19 and HOC313
254 cells, but not in OSC-20 cells or fibroblasts. Additional studies are needed to develop a
255 better understanding of the apoptosis mechanism relative to the suppression of Rac
256 activity and its related regulatory signal pathways. The end result of these efforts may
257 lead to the development and design new strategic therapeutic approaches in the
258 treatment of oral squamous cell carcinoma.

259

260 **Materials and Methods**

261 **Antibodies and chemicals**

262 Anti-Rac1 (23A8) and anti- β -actin (MAB 1501) monoclonal antibodies were purchased
263 from [Upstate Biotechnology and Chemicon International, respectively (now Merck
264 KGaA, and its affiliates), Darmstadt, Germany]. Both the anti-JNK and anti-phospho-
265 JNK (Thr183/Tyr185) polyclonal antibodies were purchased from R&D Systems, Inc.
266 (Minneapolis, MN, USA). E-cadherin (36/E-Cadherin) and N-cadherin (32/N-Cadherin)
267 were obtained from BD Biosciences (Becton Dickinson, Franklin Lakes, New Jersey,
268 USA). Cytokeratin (AE1/3) and vimentin (V9) were purchased from Dako Agilent
269 Technologies, Inc. (Santa Clara, CA, USA). Secondary antibodies were purchased from
270 Cell Signaling Technology, Inc. (Danvers, MA, USA). The complementary DNA
271 (cDNA) of the dominant negative N17Rac1 (Rac-DN), which encoded for a mutated
272 amino acid 17 from Thr to Asn was provided by Dr. A. Hall (University College
273 London, Laboratory for Molecular Cell Biology, UK). The expression plasmid was
274 constructed as previously described [22].

275

276 **Cell culture and cell treatment**

277 Three human-derived oral SCC cell lines, OSC-20, OSC-19, and HOC313 were
278 previously established and used in the study. OSC-20 cells are classified as grade 3
279 using the Y-K classification regarding mode of invasion, OSC-19 cells are classified
280 grade 4C, and HOC313 cells are classified as grade 4D. Fibroblasts cells were isolated
281 from the lip skin of adult patients. All clinical studies were approved by the Ethics
282 Committees of Osaka City University Hospital and Osaka University Dental Hospital.
283 The cancer cells including the fibroblasts were cultured in Dulbecco's modified Eagle's
284 medium (DMEM) supplemented with 10% fetal bovine serum, 5% Nu-serum Growth
285 Medium Supplement (Oscient Pharmaceuticals Corp., Waltham, Massachusetts, USA),

286 and 2 mM L-glutamine at 37°C and 5% CO₂ humidified atmosphere. The cells were
287 typically passaged when they reached 85–90% confluency. The cells were seeded into
288 6-well cell culture plates with 2 ml growth medium and any treatment was applied the
289 following day. All inhibitors were added 1 h prior to treating the cells with NSC23766.
290 Once the NSC23766 was added, the cells were incubated for 9 h. The dimethyl
291 sulfoxide (DMSO) concentrations were maintained at equal concentrations in the
292 control cells and in those receiving the inhibitors in the media. The DMSO
293 concentration never exceeded 0.1%. The three SCC cell lines were transiently
294 transfected with the expression plasmids using FuGENE HD transfection reagent
295 (Roche Molecular Systems, Inc., Upper Bavaria, Germany) according to the
296 manufacturer's instructions as described in the online link.

297

298 **Rac pull-down assay and western blotting**

299 The three SCC cell lines (OSC-20, OSC-19, and HOC313) and the fibroblasts were
300 treated with 0, 50, or 100 µM of NSC23766 and incubated for 9 h in serum. After
301 treatment, the cells were transiently transfected with Rac-DN for 48 h. The cells were
302 then lysed with 0.3 ml of a lysis buffer (25 mM Tris, pH7.5; 150 mM NaCl; 5 mM
303 MgCl₂; 1% NP-40; 1 mM DTT; and 5% glycerol), mixed well, and incubated at 4°C for
304 5 min. The lysates were carefully clarified, the protein concentrations normalized, and
305 the GTP-loaded Rac pulled down from the total protein lysates using a Rac1 Activation
306 Kit (GST-human Pak1-PBD, Thermo Fisher Scientific, Waltham, MA, USA) according
307 to the manufacturer's instructions. The precipitates were washed and boiled and the
308 proteins separated by 10% sodium dodecyl sulfate polyacrylamide gel electrophoresis
309 (SDS-PAGE). The proteins were transferred from the gels onto nitrocellulose

310 membranes and quantified by anti-Rac1 immunoblotting.

311 For western blot analysis, a RIPA Lysis Buffer system (Santa Cruz Biotechnology,
312 Inc., Dallas, Texas, USA) was used to lyse the cells and generate the cell extracts. The
313 lysates were clarified, the protein concentrations adjusted to standards amounts, and
314 boiled in 3× sample buffer. The samples were separated by SDS-PAGE, the proteins
315 were transferred onto nitrocellulose membranes. The membranes were subsequently
316 blocked with 5% membrane blocking agent (skim milk) for 1 h incubated with the
317 appropriate antibodies and then visualized using Amersham ECL Prime Western
318 Blotting Detection Reagent (GE Healthcare, Chicago, IL, USA).

319

320 **Immunofluorescence staining**

321 To detect the morphological changes of the nuclei, the cells were stained with DAPI.
322 Briefly, OSC-20, OSC-19, HOC313, and fibroblast cells were seeded (10^5 cells) onto
323 round glass coverslips, #1.5 thickness, 18 mm in 12-well tissue culture plates. The cells
324 were experimentally treated as described above and then fixed in 4% paraformaldehyde,
325 washed, and incubated with DAPI stain for 1 h at room temperature. After DAPI
326 staining, the cells were stained with rhodamine-phalloidin for 1 h at room temperature,
327 washed, and the cells adhering to the coverslips were mounted onto glass microscope
328 slides using mounting medium. An Axiovert 200M Inverted microscope (Carl Zeiss,
329 Germany) was used to visualize the cells and to capture the resulting fluorescent
330 images.

331

332 **Detection of apoptosis**

333 To detect apoptosis, we used a cell death detection ELISA (Roche Molecular Systems,

334 Inc.), which is an analytical quantitative sandwich enzyme immunoassay technique that
335 uses the interaction the mouse monoclonal antibodies with DNA and histone to detect
336 internucleosomal fragmented DNA. The test was performed according to the
337 manufacturer's instructions.

338

339 **Statistical analysis**

340 Results were presented as the means \pm standard deviations (SD), the means were
341 compared, and the fold change (effect size) was measured after treatment. Paired
342 observations were compared by paired t-test, hypothesis testing was done using 2-tailed
343 distribution, and 95% confidence intervals were provided for the tests statistics. A $p <$
344 0.05 was considered statistically significant for all tests.

345

346 **Conflict of Interest**

347 The authors declare no conflict of interest.

348

349 **Acknowledgements**

350 This work was supported by Japan Society for the Promotion of Science (JSPS) grant
351 (grant no. 20592328). Special thanks to Dr. Tomohiro Otani and Dr. Yoshimi Takai for
352 helpful discussions.

353

354 **References**

- 355 1. Parri M, Chiarugi P. Rac and Rho GTPases in cancer cell motility control. Cell
356 Commun Signal. 2010; doi: 10.1186/1478-811X-8-23.
- 357 2. Bar-Sagi D, Hall A. Ras and Rho GTPases: A family reunion. Cell. 2000; 103:

- 358 227–238.
- 359 3. Guo F, Cancelas JA, Hildeman D, Williams DA, Zheng Y. Rac GTPase isoforms
360 Rac1 and Rac2 play a redundant and crucial role in T-cell development. *Blood*.
361 2008; 112: 1767–75. doi: 10.1182/blood-2008-01-132068.
- 362 4. Li H, Peyrollier K, Kilic G, Brakebusch C. Rho GTPases and cancer. *Biofactors*.
363 2014; 40: 226–235. doi: 10.1002/biof.1155.
- 364 5. Wang RA, Li QL, Li ZS, Zheng PJ, Zhang HZ, Huang XF, et al. Apoptosis
365 drives cancer cells proliferate and metastasize. *J Cell Mol Med*. 2013; 17: 205–
366 211.
- 367 6. Matsuoka Y, Nakahara H, Nozaki S, Otani T, Kogo M. Inhibition of Rac induces
368 hyper-activation of c-Jun N-terminal kinase and caspase-dependent apoptosis.
369 *Oral Sci Int*. 2008; 5: 52–60.
- 370 7. Aznar S, Lacal JC. Rho signals to cell growth and apoptosis. *Cancer Lett*. 2001;
371 165: 1–10.
- 372 8. Zhang B, Zhang Y, Shacter E. Rac1 inhibits apoptosis in human lymphoma cells
373 by stimulating Bad phosphorylation on Ser-75. *Mol Cell Biol*. 2004; 24: 6205–
374 6214.
- 375 9. Senger DL, Tudan C, Guiot MC, Mazzoni IE, Molenkamp G, LeBlanc R, et al.
376 Suppression of Rac activity induces apoptosis of human glioma cells but not
377 normal human astrocytes. *Cancer Res*. 2002; 62: 2131–2140.
- 378 10. Stankiewicz TR, Ramaswami SA, Bouchard RJ, Aktories K, Linseman DA.
379 Neuronal apoptosis induced by selective inhibition of Rac GTPase versus global
380 suppression of Rho Family GTPases is mediated by alterations in distinct
381 mitogen-activated protein kinase signaling cascades. *J Biol Chem*. 2015; 290:

- 382 9363–9376.
- 383 11. Jin S, Ray RM, Johnson LR. TNF- α /cycloheximide-induced apoptosis in
384 intestinal epithelial cells requires Rac1-regulated reactive oxygen species. *Am J*
385 *Physiol Liver Physiol.* 2008; 294: G928–937. doi/10.1152/ajpgi.00219.2007.
- 386 12. Karlsson R, Pedersen ED, Wang Z, Brakebusch C. Rho GTPase function in
387 tumorigenesis. *Biochim Biophys Acta.* 2009; 1796: 91–98. doi:
388 10.1016/j.bbcan.2009.03.003.
- 389 13. Kamai T, Yamanishi T, Shirataki H, Takagi K, Asami H, Ito Y, et al.
390 Overexpression of RhoA, Rac1, and Cdc42 GTPases is associated with
391 progression in testicular cancer. *Clin Cancer Res.* 2004; 10: 4799–4805.
- 392 14. Baugher PJ, Krishnamoorthy L, Price JE, Dharmawardhane SF. Rac1 and Rac3
393 isoform activation is involved in the invasive and metastatic phenotype of human
394 breast cancer cells. *Breast Cancer Res.* 2005; 7: R965–974.
- 395 15. Wang W, Yang LY, Huang GW, Yang ZL, Lu WQ, Peng JX, et al.
396 Overexpression of the RhoC gene correlates with invasion and metastasis of
397 hepatocellular carcinoma. *Zhonghua Zhong Liu Za Zhi.* 2004; 26: 279–282.
- 398 16. Minden A, Lin A, Claret FX, Abo A, Karin M. Selective activation of the JNK
399 signaling cascade and c-Jun transcriptional activity by the small GTPases Rac
400 and Cdc42Hs. *Cell.* 1995; 81: 1147–1157.
- 401 17. Teramoto H, Coso OA, Miyata H, Igishi T, Miki T, Gutkind JS. Signaling from
402 the small gtp-binding proteins rac1 and cdc42 to the c-jun n-terminal kinase
403 stress-activated protein-kinase pathway - a role for mixed lineage kinase-3
404 protein-tyrosine kinase-1, a novel member of the mixed lineage kinase family. *J*
405 *Biol Chem.* 1996; 271: 27225–27228.

- 406 18. Gallagher ED, Xu S, Moomaw C, Slaughter CA, Cobb MH. Binding of
407 JNK/SAPK to MEKK1 is regulated by phosphorylation. *J Biol Chem.* 2002; 277:
408 45785–45792.
- 409 19. Yamamoto E, Kohama G-I, Sunakawa H, Iwai M, Hiratsuka H. Mode of
410 invasion, bleomycin sensitivity, and clinical course in squamous cell carcinoma
411 of the oral cavity. *Cancer.* 1983; 51: 2175–2180.
- 412 20. Joiakim A, Mathieu PA, Palermo C, Gasiewicz TA, Reiners JJ. The Jun N-
413 terminal kinase inhibitor SP600125 is a ligand and antagonist of the aryl
414 hydrocarbon receptor. *Drug Metab Dispos.* 2003; 31: 1279–1282.
- 415 21. Coleman ML, Olson MF. Rho GTPase signalling pathways in the morphological
416 changes associated with apoptosis. *Cell Death Differ.* 2002; 9: 493–504.
- 417 22. Imamura H, Takaishi K, Nakano K, Kodama A, Oishi H, Shiozaki H, et al. Rho
418 and Rab small G proteins coordinately reorganize stress fibers and focal
419 adhesions in MDCK cells. *Mol Biol Cell.* 1998; 9: 2561–2575.
- 420
- 421

Figure 1

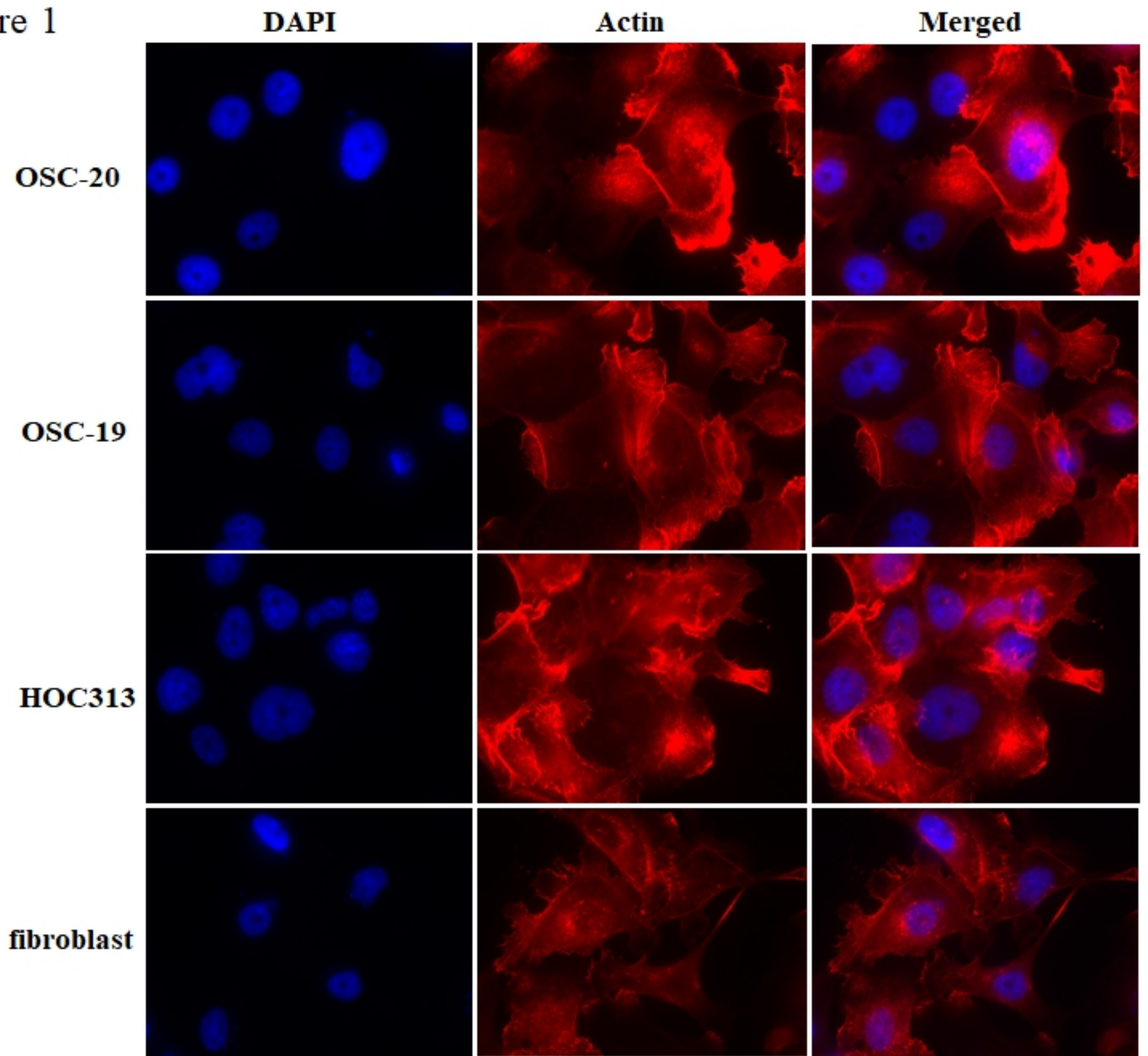


Figure 1

Figure 2

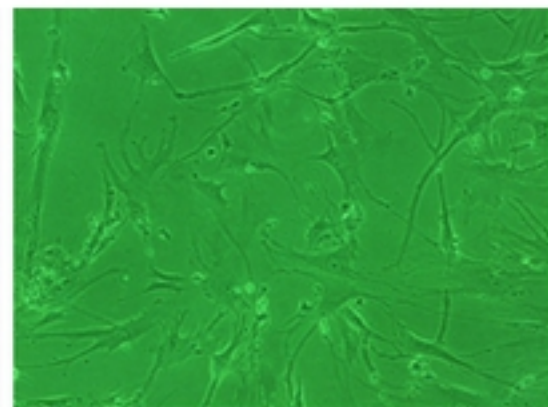
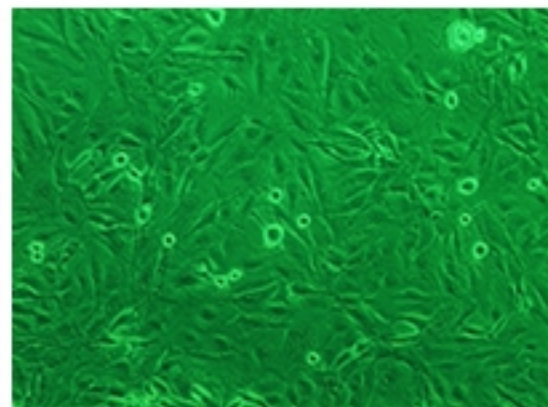
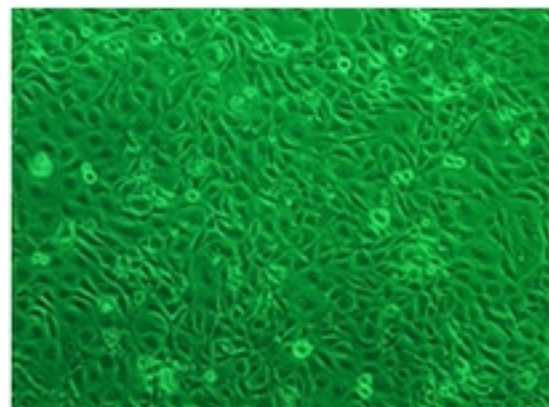
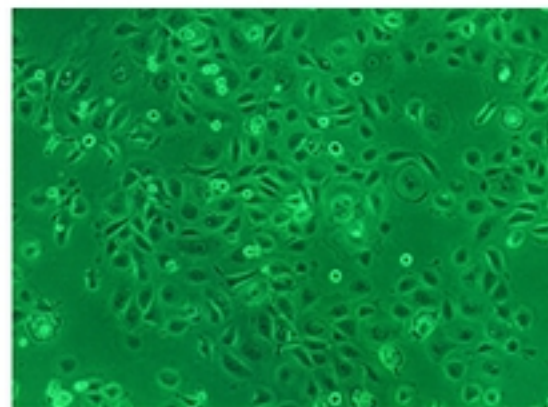
OSC-20 cells

OSC-19 cells

HOC313 cells

fibroblasts

Untreated



NSC23766 100 μ M 24h

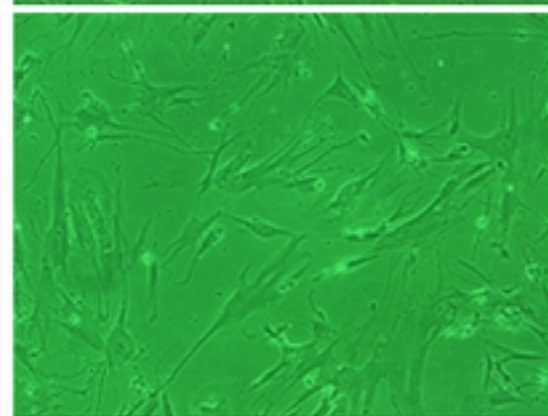
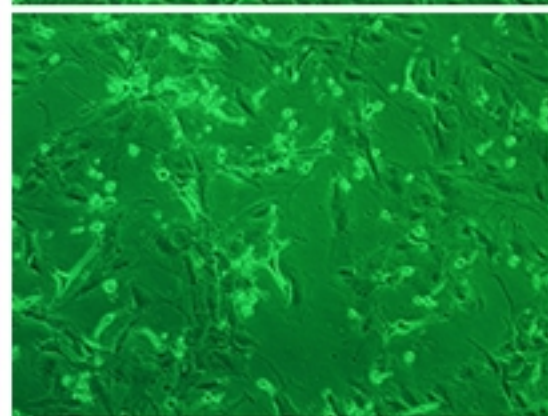
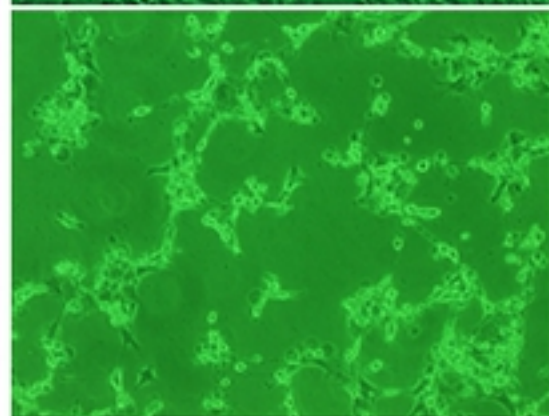
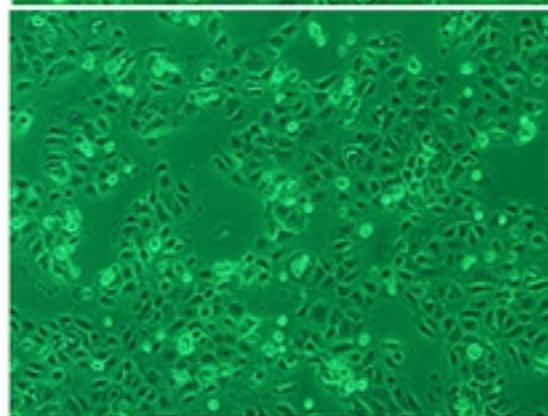


Figure 2

Figure 3

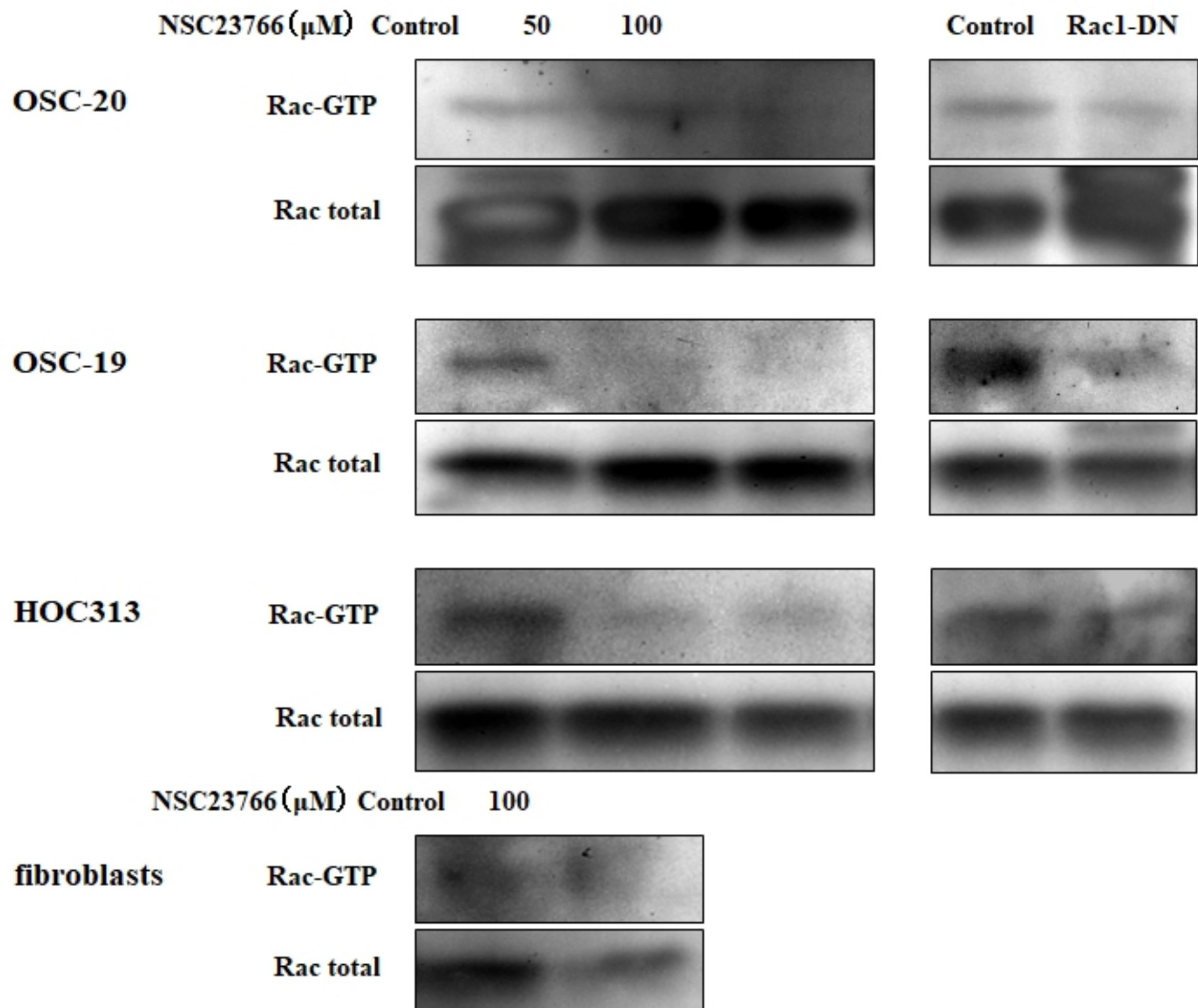


Figure 3

Figure 4

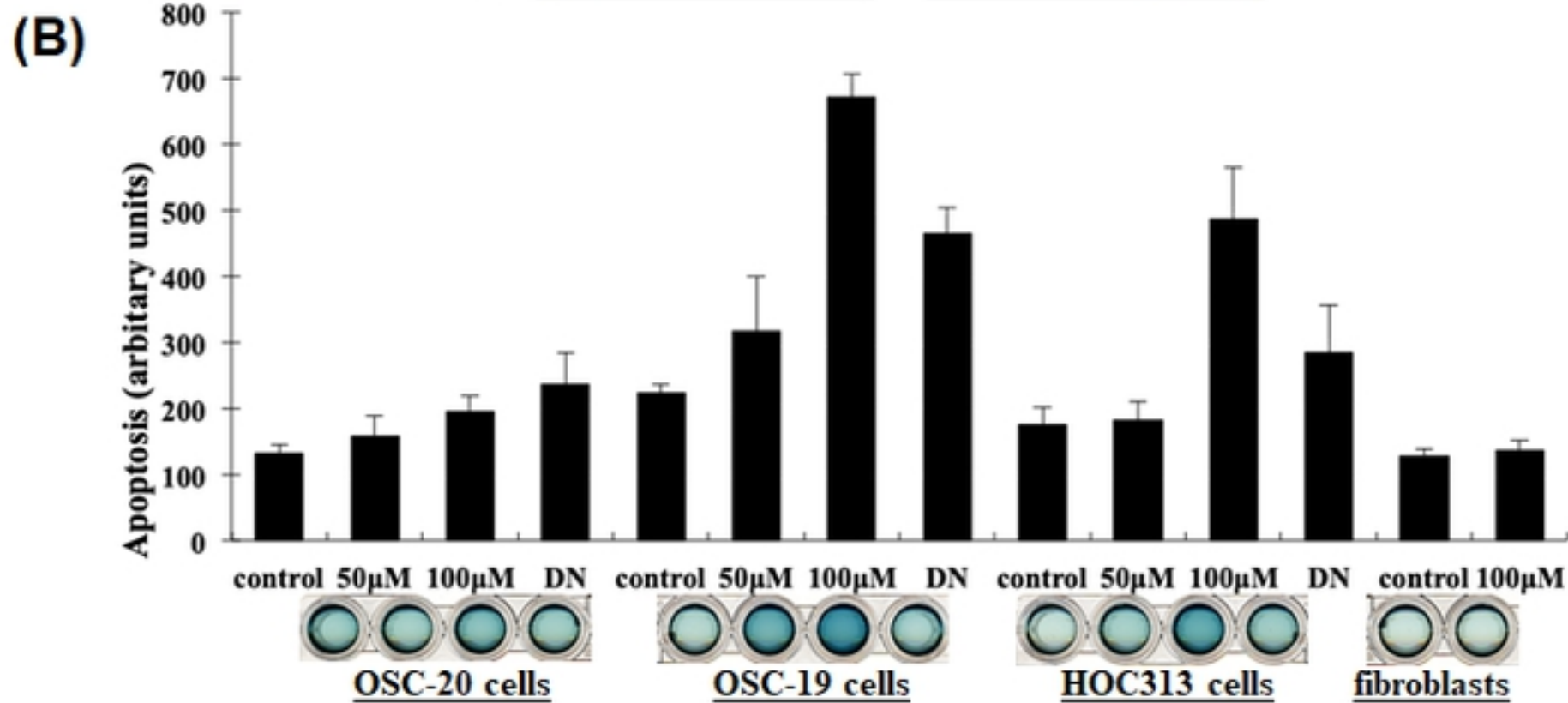
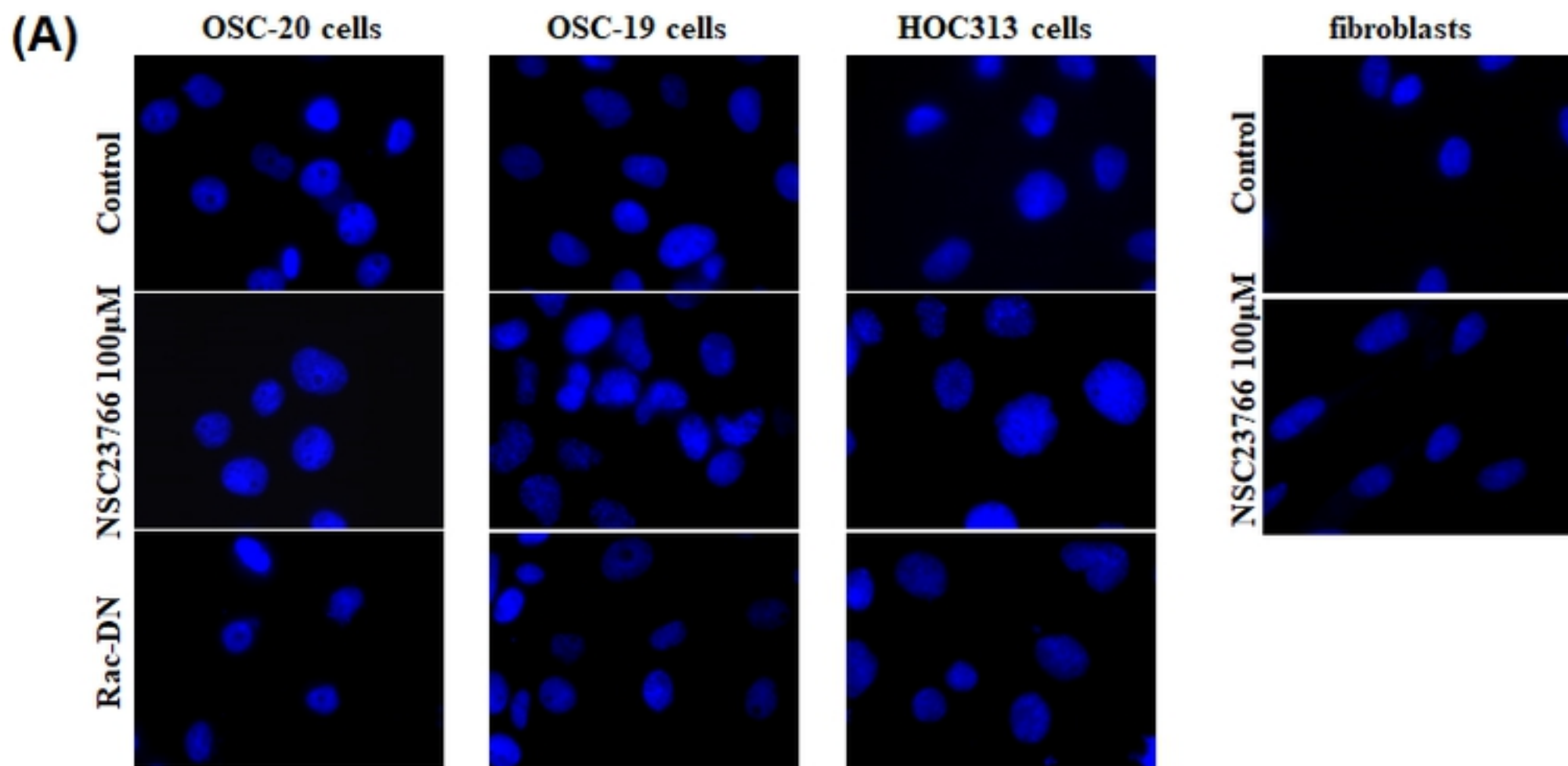


Figure 4

Figure 5

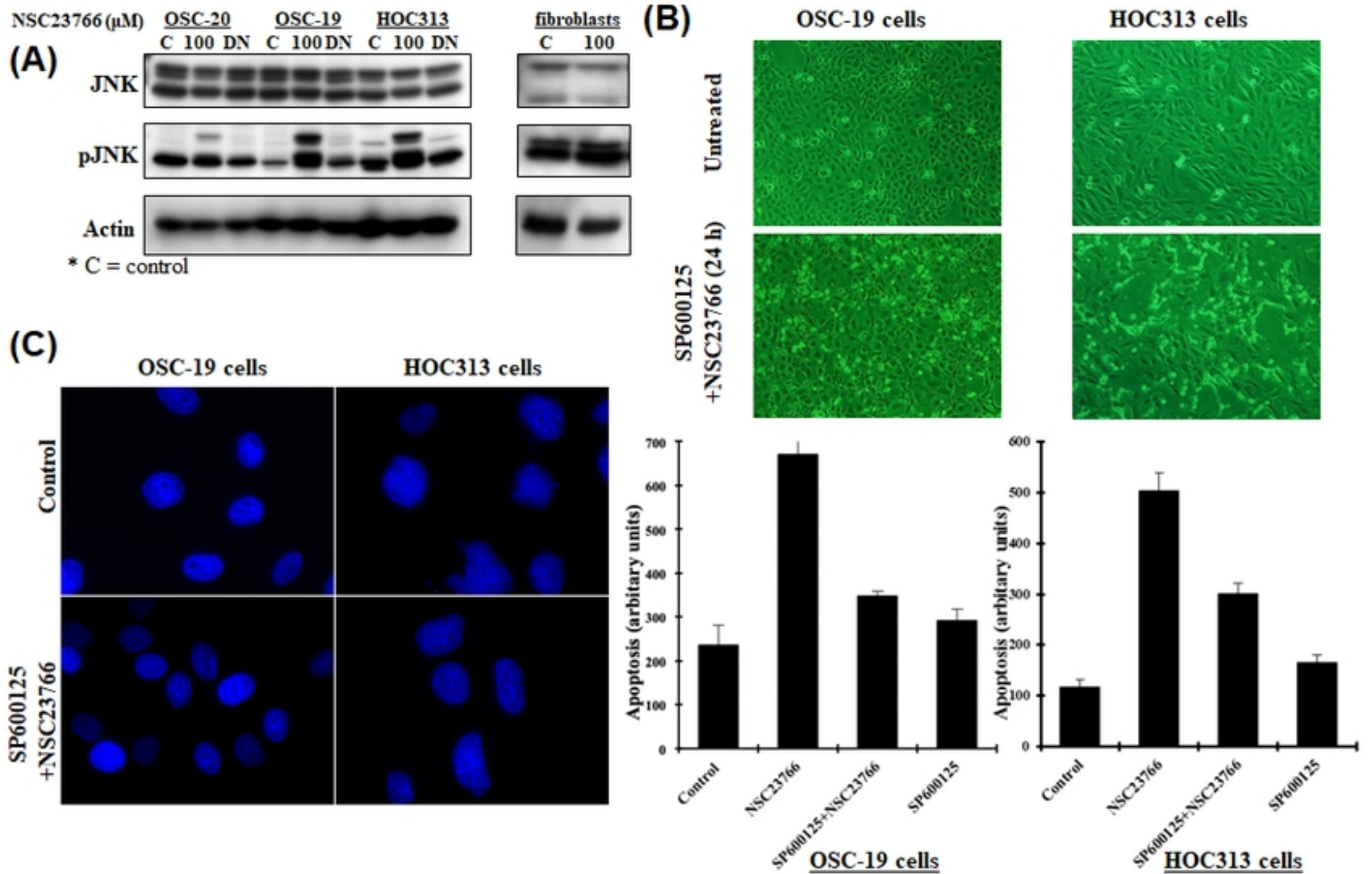


Figure 5